IEEE Photonics Journal
An IEEE Photonics Society Publication

Mitigation of Efficiency Droop in an Asymmetric GaN-Based High-Power Laser Diode With Sandwiched GaN/InAlN/GaN Lower Quantum Barrier

Volume 10, Number 06, December 2018

Tian Lan
Guangzheng Zhou
Ying Li
Congcong Wang
Zhiyong Wang

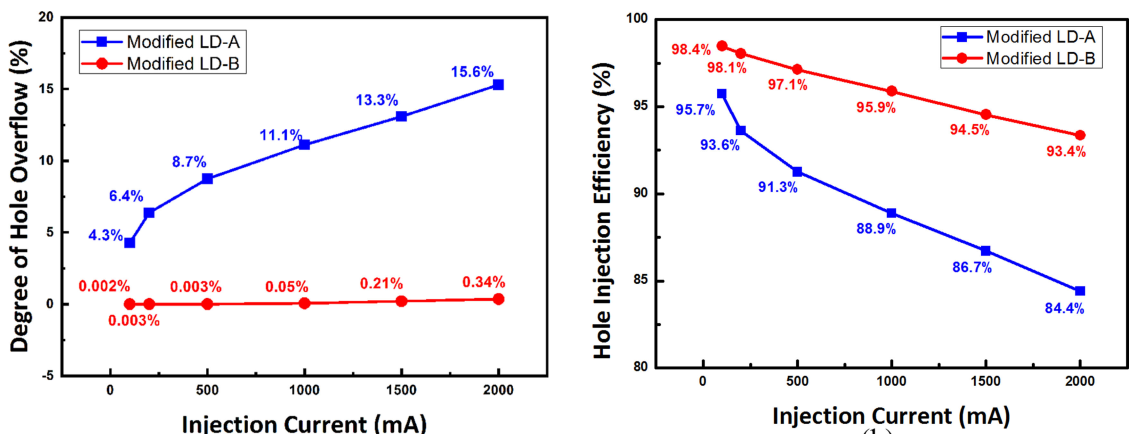

(a) (b)

DOI: 10.1109/JPHOT.2018.2878443

Mitigation of Efficiency Droop in an Asymmetric GaN-Based High-Power Laser Diode With Sandwiched GaN/InAlN/GaN Lower Quantum Barrier

Tian Lan, Guangzheng Zhou, Ying Li, Congcong Wang, and Zhiyong Wang

Institute of Laser Engineering, Beijing University of Technology, Beijing 100124, China

DOI:10.1109/JPHOT.2018.2878443

Manuscript received October 4, 2018; revised October 20, 2018; accepted October 23, 2018. Date of publication October 30, 2018; date of current version November 13, 2018. Corresponding author: Zhiyong Wang (e-mail: zywang_bjut@126.com).

Abstract: The phenomenon of efficiency droop is comprehensively investigated in an asymmetric GaN-based laser diode (LD). Numerical simulations and experiments are both conducted. It is found that with the introduction of a sandwiched GaN/InAlN/GaN lower quantum barrier (LQB) instead of the bulk GaN LQB in an asymmetric GaN-based high-power blue LD, the efficiency droop is effectively mitigated to only 9.7% under continuous-wave operation with no degradation in the crystal quality. Compared with the conventional asymmetric GaN-based LD, the wall-plug efficiency is successfully increased by 24.7% from 15.8% to 19.7% at high injection current of 2000 mA, promoting the increase of slope efficiency and output power, while the threshold current is reduced by 15.2%. These improvements are primarily attributed to the inserted high-quality InAlN thin barrier layer, which could form an extra potential barrier beneath the first InGaN quantum well to remarkably alleviate the hole overflow from the active region and enhance the radiative recombination rate.

Index Terms: Asymmetric GaN LD, efficiency droop, hole overflow, wall-plug efficiency.

1. Introduction

Over the past two decades, the wide bandgap InGaN/GaN based light emitting diodes (LEDs) and laser diodes (LDs) have attracted increasing attentions all over the world and shown great potentials in next-generation lighting applications, such as white-light sources, ultraviolet LEDs, laser display, laser TV, car laser light [1]–[5], because of the high thermal conductivity, promising optoelectronics characters, great reliability, high energy efficiency. However, one of the critical factors that hinder the further development of the high-power GaN-based LDs and remain unsolved is the well-known efficiency droop effect [6], [7], and it is becoming more and more severe with the increase of injection current. The reasons that deteriorate the performance of high-power LDs through efficiency droop are proved to be the carrier leakage from the active region [8], Auger recombination [9], lattice-mismatch-induced piezoelectric polarization field [10] and self-heating [11]. Recently, some research groups have proposed a new kind of GaN-based LDs with asymmetric InGaN/GaN multiple quantum wells (MQWs) [12], [13]. Compared with the conventional symmetric LDs, the asymmetric GaN-based LDs demonstrate a better opto-electrical performance with improved internal quantum efficiency (IQE) and suppressed efficiency droop effect due to the increase of the optical confinement factor. However, a significant degradation of carrier injection efficiency (CIE) into the InGaN/GaN active region still exists at high injection current. Except that, a plenty of methods have also been put forward to effectively solve the negative influence of the electron leakage in order to achieve high performance GaN-based LDs, such as the introduction of AlGaN/InGaN superlattice (SL) EBL [14], [15], high quality InAlGaN EBL [16]–[18], lattice-matched InAlN EBL [19], the experiment results are all satisfying. On the contrary, the hole overflow, which is another key factor that affects the radiative recombination rate of the LEDs and LDs, is often neglected. Most of the related investigations of hole overflow are just concentrated on the ultraviolet LED because of its shallower quantum well [20]. However, a considerable level of hole overflow could still be detected in the blue/green laser devices [21], [22]. Some researchers have suggested to adopt multi-barrier to replace the bulk GaN barrier layer so as to enhance the carrier confinement in the active region and improve the device performance, such as AlGaN/GaN barrier layer [23], [24], InAlGaN barrier layer [25] and compositionally step-graded InGaN barrier [26]. However, one big problem is that good quality of AlGaN layer usually need growth temperature as high as 1000°C. As a result, the crystal quality of InGaN QWs would be damaged with high possibility, which may have counter-productive effect on the performance of opto-electric devices, especially at high injection current. Besides, the replacement of all GaN barriers by using InAlGaN layer may deteriorate the optical confinement in the MQWs [27], since using InGaN layer as the quantum barrier (QB) is often considered as an important method to increase the optical confinement in MQWs.

In this paper, a new asymmetric GaN-based high-power blue LD designed with a sandwiched GaN/InAlN/GaN lower quantum barrier (GIG-LQB) structure with good quality instead of the bulk GaN LQB is proposed and fabricated. Systematical investigations are carried out by means of numerical simulations and experiments. In comparison with the conventional asymmetric GaN-based blue LD, the new proposed LD exhibits a much improved CIE and radiative recombination rate at high injection current due to the alleviated hole overflow and enhanced carrier confinement in the active region. As a result, the final wall-plug efficiency (WPE) is increased by 24.7% from 15.8% to 19.7% at high injection current of 2000 mA, and the phenomenon of efficiency droop is also effectively mitigated to only 9.7%.

2. Experimental Details

Two asymmetric GaN-based LD structures were grown on 2-inch c-plane freestanding GaN (FS-GaN) substrates with original threading dislocation (TD) density of $5 \times 10^6/\text{cm}^2$ using a commercial Metalorganic Chemical Vapor Deposition (MOCVD) system. Trimethylgallium (TMGa), triethylgallium (TEGa), trimethylindium (TMIn), trimethylaluminum (TMAl) and ammonia (NH3) were used as Ga, In, Al and N precursors, respectively. N_2 and H_2 were both used as carrier gases at different growth stages. Silane (SiH4) and bis(cyclopentadienyl)magnesium (Cp2Mg) were used as the n-type and p-type doping sources, respectively. The detailed schematic structural diagrams of the two LD structures are shown in Fig. 1. The two LDs share approximately the identical structure, except for the asymmetric InGaN/GaN active region. The conventional asymmetric InGaN/GaN active region of LD-A consists of 15-nm-thick GaN LQB, two undoped 3-nm-thick $In_{0.23}GaN$ QWs separated by 5-nm-thick undoped $In_{0.02}GaN$ QBs. And the proposed InGaN/GaN active region of LD-B employs a sandwiched GaN (5 nm)/$In_{0.15}Al_{0.85}N$ (5 nm)/GaN (5 nm) multi-layers LQB to replace the bulk GaN LQB, and the thin $In_{0.15}Al_{0.85}N$ layer is designed to be a little lattice-mismatched with GaN layer in order to bring in extra tensile strain to compensate the compressive strain induced by lower InGaN waveguiding (WG) layer and upper $In_{0.23}GaN$ QWs. And the rest layers of the two LDs remain identical, which include a 3-μm-thick Si-doped GaN layer directly grown on the FS-GaN substrate, a 1-μm-thick Si-doped $Al_{0.12}GaN$ lower cladding layer, a 40-nm-thick Si-doped GaN layer, a 180-nm-thick Si-doped $In_{0.05}GaN$ waveguiding layer, an 180-nm-thick undoped $In_{0.05}GaN$ upper waveguiding layer, a 15-nm-thick Mg-doped $Al_{0.2}GaN$ electron blocking layer (EBL), a 500-nm-thick Mg-doped $Al_{0.06}GaN$ upper cladding layer and a 20-nm-thick heavily Mg-doped GaN contact layer. Pd/Pt/Au were applied for the p-type electrode, while Ti/Al/Ti/Pt/Au were the n-type electrode. Finally, the LDs were fabricated into ridge-waveguide lasers (RWG) using a self-aligned ridge technique

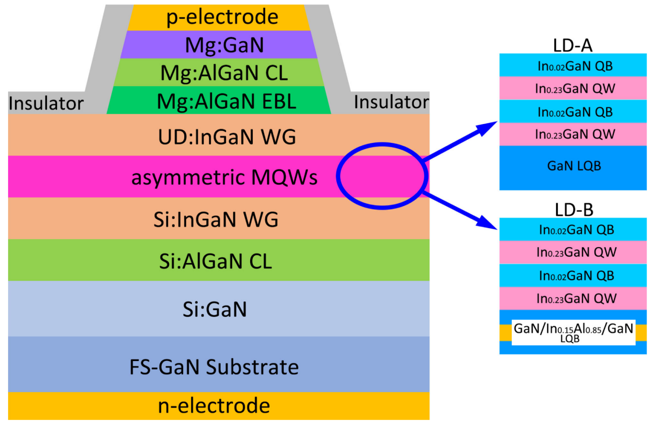

Fig. 1. Schematic diagrams of the two blue LDs with different asymmetric active region grown on FS-GaN substrate.

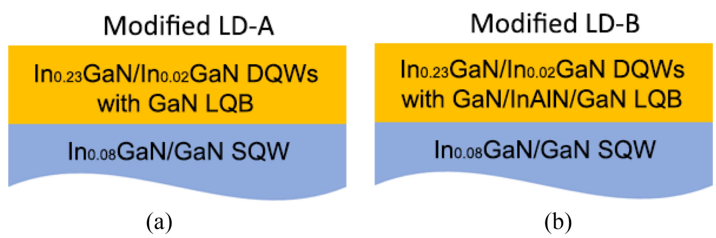

Fig. 2. The schematic diagram of the two modified LD structures with In0.08GaN/GaN single quantum well (SQW) hole overflow detector beneath the original active region.

with 1.2 mm cavity length and 15 μm ridge width in order to obtain high power output. The rear facet was coated with 95% high reflection film, while the front facet was coated with 5% anti-reflection film. After the whole chip process, the two LDs were mounted on a heat sink with good thermal conductivity for following tests.

Al/In concentrations were determined and calibrated by high-resolution X-ray diffraction (HRXRD). And L-I-V characters were measured by the Thorlabs current source meter and power meter. And the two-dimensional LASTIP simulation software, developed by the Crosslight Software Inc, was employed for the numerical simulation of carrier distribution. The morphology was characterized by a Bruker Dimension Edge atomic force microscope (AFM) in tapping mode.

3. Results and Discussion

3.1 Simulation Results

To facilitate the observation and theoretical calculation of the degree of hole overflow (DHO) from the asymmetric $In_{0.23}GaN/In_{0.02}GaN$ active region of both LDs, the two original structures are modified during the simulation process by adding an extra $In_{0.08}GaN/GaN$ single quantum well (SQW) prior to the original active region as shown in Fig. 2, respectively, which works as a hole overflow detector. Additionally, the direct bandgap energy of InGaN, AlGaN and InAlN material used in our simulations are calculated by using the following formulas [28]:

$$E_g\left(In_xGa_{1-x}N\right) = 0.71x + 3.44\left(1 - x\right) - 1.34x\left(1 - x\right) \tag{1}$$

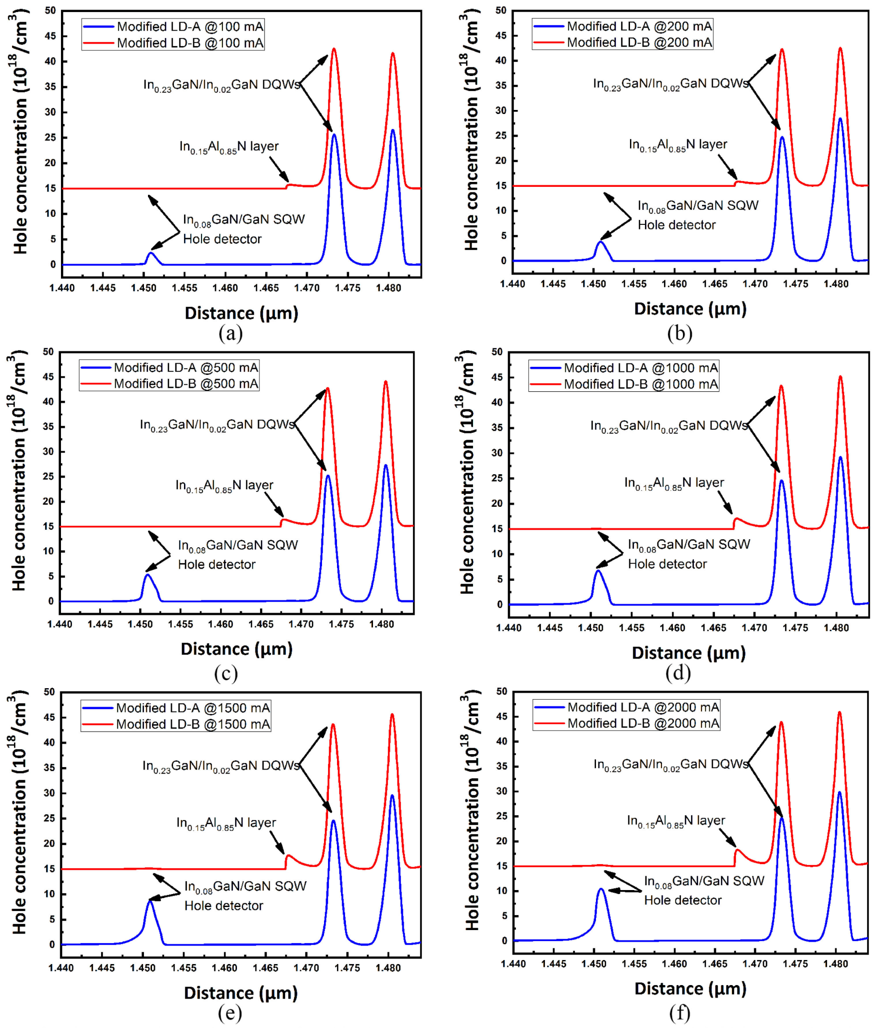

Fig. 3. Plots of hole distributions of the modified LD-A and B under the injection current of (a) 100 mA, (b) 200 mA, (c) 500 mA, (d) 1000 mA, (e) 1500 mA, (f) 2000 mA, respectively.

$$E_g\left(Al_xGa_{1-x}N\right) = 6.14x + 3.44\,(1-x) - 0.7x\,(1-x) \quad (2)$$

$$E_g\left(In_xAl_{1-x}N\right) = 0.71x + 6.14\,(1-x) - 3.4x\,(1-x) \quad (3)$$

During the simulation, the screening factor of polarization was set to be 0.25. Ohmic contact was also applied for both p-type contact and n-type contact. As shown in Fig. 3(a)–(f), the simulated hole distributions of the modified LD-A and LD-B were plotted as a function of the injected current by solving the Poisson's equation self-consistently and the current continuity equations. The right two peaks represent the hole concentration confined in the original asymmetric $In_{0.23}GaN/In_{0.02}GaN$ double quantum wells (DQWs), while the left single peak stands for the hole overflow concentration detected by the inserted $In_{0.08}GaN/GaN$ SQW. It shows that the hole overflow for both LD structures are becoming more and more severe with the injection current increasing from 100 mA (low injection) to 2000 mA (high injection). However, the hole overflow is much more serious in the modified LD-A since the very beginning, while in the modified LD-B the phenomenon of hole overflow is almost completely eliminated until the injection current exceeds 1500 mA. And the hole leaked from the

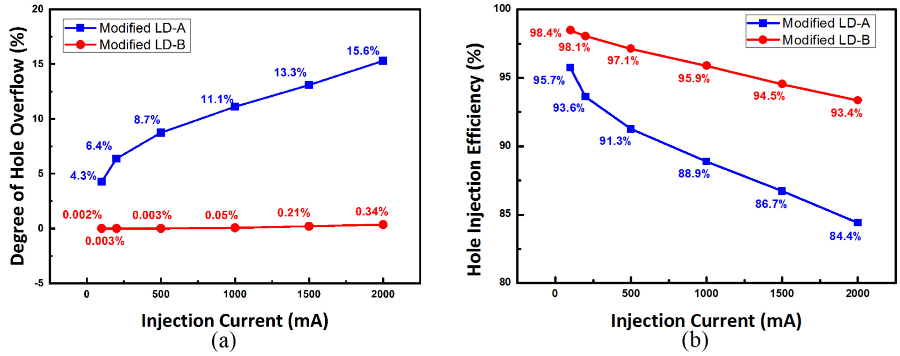

Fig. 4. Plot of (a) degree of hole overflow (DHO) and (b) hole injection efficiency (HIE) as a function of injection current.

active region could be blocked by the inserted $In_{0.15}Al_{0.85}N$ thin barrier layer, which could form a higher barrier on the valence band to weaken the hole overflow, and thus a small number of holes tend to accumulate near the first $In_{0.23}GaN$ QW, this is the reason why there is a small peak before first QW.

By extracting the value of hole concentration peaks from simulation results, the DHO and hole injection efficiency (HIE) are precisely calculated and depicted in Fig. 4, respectively. As shown in Fig. 4(a), the DHO of the modified LD-B is calculated to be 0.34% at the high injection current of 2000 mA, which is significantly reduced compared with the 15.3% DHO of modified LD-A. And at low injection current, the DHO of LD-B is almost totally diminished, while the minimum DHO of LD-A is 4.3% at 100 mA, which could still affect the radiative recombination rate. Fig. 4(b) shows the HIE as a function of the injected current. It is proved that even though a certain number of holes are blocked and accumulated near the first InGaN QW due to the middle-inserted InAlN thin barrier, the HIE of LD-B is still increased by 10.6%, up to 93.4%, at 2000 mA injection current, while the HIE of LD-A is only 84.4% due to the large hole overflow. Even though the hole injection efficiencies for both LDs are gradually reduced with the increase of injection current, which is mainly attributed to the stronger quantum confinement starks effect (QCSE), the decrement of HIE is 11.8% for LD-A and 5.1% for LD-B, indicating that the LD structure with GIG-LQB owns a more stabilized performance. Therefore, it is theoretically confirmed that by inducing a sandwiched GIG-LQB instead of the pure GaN LQB, the hole overflow can be effectively mitigated, leading to an enhancement of radiative recombination and suppression of efficiency droop effect, especially at high injection current.

3.2 Experiment Results

The 5×5 μm^2 AFM images of LD-A and LD-B after the deposition of LQB are shown in Fig. 5 with corresponding root-mean-square (RMS) roughness values to investigate the impact of the GIG-LQB on the surface morphologies. Three test spots were chosen at an interval of 15 mm along the radial direction of each wafer. It is indicated that the typical V-shaped defects, as circled in white, still can be observed on the surface of LD-A even though the FS-GaN substrate is employed. The average threading dislocation (TD) density is calculated to be around $8 \times 10^6/cm^2$, which is higher than the TD density of the original FS-GaN substrate. Generally, the primary contributor to the degraded surface quality is the underlying thick Si-doped $In_{0.05}GaN$ lower waveguiding layer with poor crystal quality. However, not like the LD-A, no V-pits can be detected in the 5×5 μm^2 scan area of LD-B, and much flatter surface with clear atomic steps is obtained. The RMS surface roughness of each test point is 0.37 nm, 0.33 nm, 0.27 nm, respectively, which is also smaller than that of LD-A. Since inner stress is one of the main reasons that forms the V-pits in the MQWs [29], [30], the introduction of the lattice-mismatched $In_{0.15}Al_{0.85}N$ could provide an extra tensile stress to effectively compensate the large compressive stress induced by the InGaN layer. It has been reported that to increase the light output power of the GaN-based LEDs, the size of the V-pits is

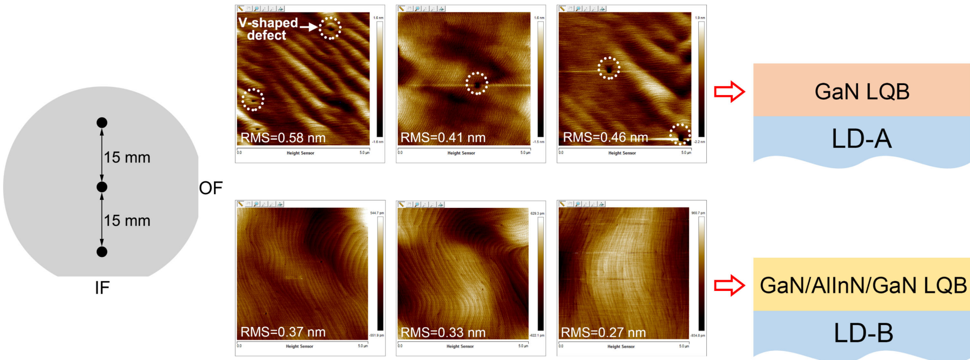

Fig. 5. Top-view 5 × 5 μm^2 AFM images of the surface morphology for LD-A and LD-B after the deposition of the LQB. Three test point were chosen for each sample with a fixed interval of 15 mm on the radial direction of the 2-inch FS-GaN substrate. And the V-shaped defects are circles in white.

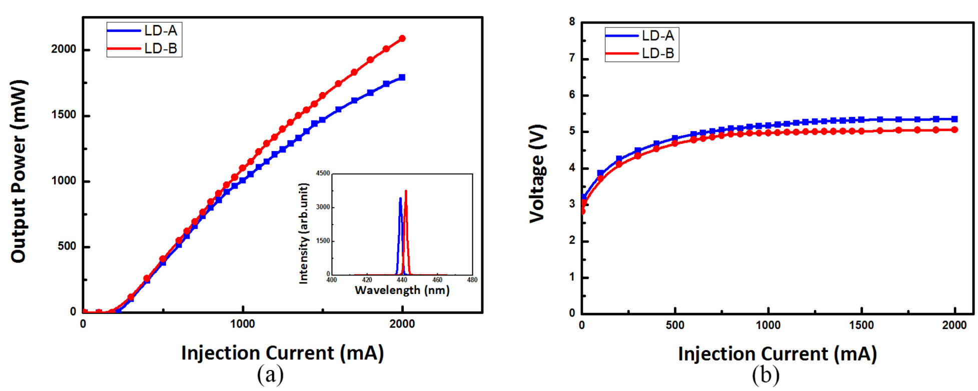

Fig. 6. Typical (a) I-L and (b) I-V characteristics under CW operation at room temperature (T = 300 K). the inset shows the emission wavelength of the two LDs.

usually enlarged on purpose to improve the light extraction efficiency (LEE) [31]. However, due to the huge difference of the injection current density between GaN-based LED and LD, the density of V-pits needs to be eliminated as much as possible in the LD devices in order to avoid the extra heat generation. As we know, the IQE is generally defined below by the injection efficiency and radiation efficiency [6],

$$\eta_{IQE} = \eta_{inj} \times \eta_{rad} = \frac{I_{qw}}{I_{tot}} \times R \frac{Bn^2}{An + Bn^2 + Cn^3} \tag{4}$$

where the first term η_{inj} is the injection efficiency into the InGaN QWs, which is significantly enhanced according to the simulation result due to the suppressed hole overflow by using GIG-LQB, and the second term η_{rad} is the radiative efficiency of the injected carriers in the QWs. In η_{rad}, the introduced factor R represents the ratio of screen carriers by the V-pits to the total injected carrier density into the QWs, which can be used to evaluate the influence of the carrier reduction by the TDs. And An is the non-radiative recombination rate or the SRH recombination rate, Bn^2 is the radiative recombination rate and Cn^3 is the Auger recombination rate. As a result, the non-radiative recombination rate could be reduced due to the decreased TD density since these V-pits usually work as the non-radiative recombination centers (NRCs) for the carriers, leading to an enhancement of electron capture rate of the active region, the electron-hole recombination rate, IQE. These advantages would be beneficial to the improvement of the final output power from the fabricated LD devices and also a longer working lifetime due to the less self-heating.

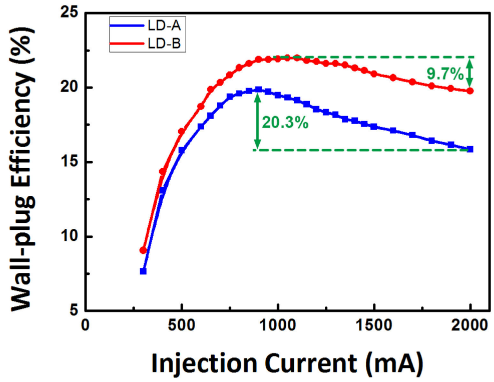

Fig. 7. Plot of the calculated wall-plug efficiency (WPE) evolution as a function of injection current after lasing.

Fig. 6 displays the typical optical and electrical characteristics for the two LDs under continuous-wave operation up to 2000 mA at room temperature (T = 300 K). As shown in Fig. 6(a), the corresponding threshold current (I_{th}) of LD-A is measured to be 223 mA, and with the introduction of GIG-LQB in LD-B the threshold current decreases by 15.2% to 189 mA. And the operation voltage is also slightly reduced, as depicted in Fig. 6(b). Some literature have reported that TDs can assist the diffusion of the point defects and impurities into the InGaN/GaN active region, especially at high junction temperature, thus causing a huge increase in the threshold current and the dramatical drop in the IQE [32], [33]. Therefore, by suppressing the generation of the TDs using high crystal quality GIG-LQB, the electrical properties are successfully improved. On the other hand, the output power of LD-B is as high as 2.1 W at the injection current of 2000 mA, which is 16.5% higher than that of LD-A. The corresponding WPE is also increased by 24.7% from 15.8% to 19.7% at injection current of 2000 mA. Moreover, efficiency droop effect is obviously mitigated in LD-B with only 9.7% decrement until the current reaches as high as 2000 mA, while LD-A exhibits an obvious efficiency droop after the injection current exceeds 1000 mA with 20.3% decrement, as displayed in Fig. 7. It reveals that the employment of a thin $In_{0.15}Al_{0.85}N$ layer with higher potential energy barrier is an effective approach to alleviate the efficiency droop by suppressing the hole overflow, increasing the carrier concentration in the QWs and enhancing the radiative recombination.

4. Conclusion

In summary, an asymmetric GaN-based high-power LD with a sandwiched GIG-LQB is fabricated on FS-GaN substrate, and the impact on the efficiency droop effect has been systematically investigated. According to the numerical simulation results, the GIG-LQB LD shows a better suppression of the hole overflow from the blue DQWs and higher CIE with the current varied from low-injection (100 mA) to high-injection (2000 mA), compared with the conventional asymmetric LD, due to the increase of the effective band offset between QW and QB by the large bandgap $In_{0.15}Al_{0.85}N$ barrier layer. As a result, the radiative recombination rate and optical output power are both significantly improved, as demonstrated by the experimental results. Meanwhile, the insertion of good quality $In_{0.15}Al_{0.85}N$ layer in the bulk GaN LQB could also leads to the reduction of V-pits density and much smoother surface morphology after the growth of GIG-LQB, which is quite beneficial for the deposition of the rest layers and enhancement of the electron-hole recombination rate in the active region. Finally, the phenomenon of efficiency droop is successfully mitigated from 20.3% to 9.7% at the high injection current of 2000 mA, which provides a new approach to fabricate a more practical GaN-based LD device structure for further improvement.

References

[1] S. Masui, Y. Nakatsu, D. Kasahara, and S. Nagahama, "Recent improvement in nitride lasers," *Proc. SPIE*, vol. 10104, 2017, Art. no. 101041H.
[2] J. Yang *et al.*, "Highly uniform white light-based visible light communication using red, green, and blue laser diodes," *IEEE Photon. J.*, vol. 10, no. 2, Apr. 2018, Art. no. 8200508.
[3] I. Akasaki, "GaN-based p-n junction blue-light-emitting devices," *Proc. IEEE*, vol. 101, no. 10, pp. 2200–2210, Oct. 2013.
[4] M. Murayama *et al.*, "Watt-class green (530 nm) and blue (465 nm) laser diodes," *Physica Status Solidi (a)*, vol. 215, 2018, Art. no. 1700513.
[5] S. M. Sadaf *et al.*, "An AlGaN core-shell tunnel junction nanowire light-emitting diode operating in the ultraviolet-C band," *Nano Lett.*, vol. 17, pp. 1212–1218, 2017.
[6] J. Piprek, "Efficiency droop in nitride-based light-emitting diodes," *Physica Status Solidi (a)*, vol. 207, pp. 2217–2225, 2010.
[7] Y. Zhao, H. Fu, G. T. Wang, and S. Nakamura, "Toward ultimate efficiency: Progress and prospects on planar and 3D nanostructured nonpolar and semipolar InGaN light-emitting diodes," *Adv. Opt. Photon.*, vol. 10, pp. 246–308, 2018.
[8] J. Hengsteler, P. Prajoon, and D. Nirmal, "Analysis of high efficiency InGaN multiple-quantum-well light-emitting-diodes using InGaN step-graded barriers," *J. Nanoelectron. Optoelectron.*, vol. 13, pp. 939–943, 2018.
[9] I. S. Romanov, I. A. Prudaev, and V. V. Kopyev, "Internal quantum efficiency of led structures at various charge carrier distributions over InGaN/GaN quantum wells," *Russian Phys. J.*, vol. 61, pp. 211–215, 2018.
[10] H. Y. Ryu, K. S. Jeon, M. G. Kang, H. K. Yuh, Y. H. Choi, and J. S. Lee, "A comparative study of efficiency droop and internal electric field for InGaN blue lighting-emitting diodes on silicon and sapphire substrates," *Sci. Rep.*, vol. 7, 2017, Art. no. 44814.
[11] J. Piprek, "Internal power loss in GaN-based lasers: Mechanisms and remedies," *Opt. Quantum Electron.*, vol. 49, 2017, Art. no. 329.
[12] J. Yang *et al.*, "Performance of InGaN based green laser diodes improved by using an asymmetric InGaN/InGaN multi-quantum well active region," *Opt. Exp.*, vol. 25, pp. 9595–9602, 2017.
[13] Y. D. Lin *et al.*, "M-plane pure blue laser diodes with p-GaN/n-AlGaN-based asymmetric cladding and InGaN-based wave-guiding layers," *Appl. Phys. Lett.*, vol. 95, 2009, Art. no. 081110.
[14] S. M. Zeng, S. W. Zheng, and G. H. Fan, "Numerical investigation of InGaN light-emitting diode with Al/In-graded p-AlGaN/InGaN superlattice electron-blocking layer," *J. Electron. Mater.*, vol. 46, pp. 1100–1106, 2017.
[15] C. T. Yu, W. C. Lai, C. H. Yen, and S. J. Chang, "Effects of InGaN layer thickness of AlGaN/InGaN superlattice electron blocking layer on the overall efficiency and efficiency droops of GaN-based light emitting diodes," *Opt. Exp.*, vol. 22, no. 3, pp. A663–A670, 2014.
[16] A. J. Tzou *et al.*, "High-performance InGaN-based green light-emitting diodes with quaternary InAlGaN/GaN superlattice electron blocking layer," *Opt. Exp.*, vol. 24, pp. 11387–11395, 2016.
[17] V. Pendem, S. Adhikari, M. Mathew, S. Singh, and S. Pal, "Droop-multimode trade-off in GaN-InGaN LEDs: Effect of polarization-matched AlInGaN blocking layers," *Superlattices Microstruct.*, vol. 88, pp. 344–353, 2015.
[18] D. Robidas and D. Arivuoli, "Simulation studies of InGaN based light-emitting diodes to reduce electron overflow problem by designing electron blocking layer," *J. Nanosci. Nanotechnol.*, vol. 15, pp. 4414–4420, 2015.
[19] J. H. Tong, B. J. Zhao, Z. W. Ren, X. F. Wang, X. Chen, and S. T. Li, "InGaN-based blue light emitting diodes with AlInN-GaN-AlInN electron blocking layers," *Chin. Phys. Lett*, vol. 30, 2013, Art. no. 058503.
[20] Y. Xing *et al.*, "Suppression of hole leakage by adding a hole blocking layer prior to the first quantum barrier in GaN-based near-ultraviolet laser diodes," *Physica Status Solidi (a)*, vol. 214, 2017, Art. no. 1700320.
[21] D. S. Sizov, "Impact of carrier transport on aquamarine-green laser performance," *Appl. Phys. Exp.*, vol. 3, 2010, Art. no. 122101.
[22] Y. Cheng *et al.*, "Suppression of recombination in waveguide in c-plane InGaN-based green laser diodes," *Superlattices Microstruct.*, vol. 111, pp. 1121–1125, 2017.
[23] Y.-Y. Zhang and G.-R. Yao, "Performance enhancement of blue light-emitting diodes with AlGaN barriers and a special designed electron-blocking layer," *J. Appl. Phys.*, vol. 110, 2011, Art. no. 093104.
[24] C. Jia, T. Yu, X. Feng, K. Wang, and G. Zhang, "Performance improvement of GaN-based near-UV LEDs with InGaN/AlGaN superlattices strain relief layer and AlGaN barrier," *Superlattices Microstruct.*, vol. 97, pp. 417–423, 2016.
[25] G. Liu, J. Zhang, C. K. Tan, and N. Tansu, "Efficiency-droop suppression by using large-bandgap AlGaInN thin barrier layers in InGaN quantum-well light-emitting diodes," *IEEE Photon. J.*, vol. 5, no. 2, Apr. 2013, Art. no. 2201011.
[26] C. C. Pan, Q. Yan, H. Fu, and Y. Zhao, "High optical power and low-efficiency droop blue light-emitting diodes using compositionally step-graded InGaN barrier," *Electron. Lett.*, vol. 51, pp. 1187–1189, 2015.
[27] J. Yang *et al.*, "Suppression the leakage of optical field and carriers in GaN-based laser diodes by using InGaN barrier layers," *IEEE Photon. J.*, vol. 10, no. 4, Aug. 2018, Art. no. 1503107.
[28] P. Prajoon, M. A. Menokey, J. C. Pravin, J. Ajayan, S. Rajesh, and D. Nirmal, "Investigation of efficiency enhancement in InGaN MQW LED with compositionally step graded GaN/InAlN/GaN multi-layer barrier," *Superlattices Microstruct.*, vol. 116, pp. 71–78, 2018.
[29] Y. Chen *et al.*, "Pit formation in GaInN quantum wells," *Appl. Phys. Lett.*, vol. 72, pp. 710–712, 1998.
[30] J. Kim *et al.*, "Influence of V-pits on the efficiency droop in InGaN/GaN quantum wells," *Opt. Exp.*, vol. 22, pp. A857–A866, 2014.
[31] K. Koike *et al.*, "Improvement of light extraction efficiency and reduction of leakage current in GaN-based LED via V-pit formation," *IEEE Photon. Technol. Lett.*, vol. 24, no. 6, pp. 449–451, Mar. 2012.
[32] S. Tomiya, T. Hino, S. Goto, M. Takeya, and M. Ikeda, "Dislocation related issues in the degradation of GaN-based laser diodes," *IEEE J. Sel. Topics Quantum Electron.*, vol. 10, no. 6, pp. 1277–1286, Nov./Dec. 2004.
[33] L. Marona *et al.*, "Degradation mechanisms in InGaN laser diodes grown on bulk GaN crystals," *Appl. Phys. Lett.*, vol. 88, 2006, Art. no. 201111.